Approximate analytical solution and laboratory experiments for dam-break wave tip region in triangular channels

Bo Wang[1], Fengjie Zhang[2], Xin Liu[3], Yakun Guo[4], Jianmin Zhang[5] and Yong Peng[6]

[1]Professor, State Key Laboratory of Hydraulics and Mountain River Engineering, College of Water Resource and Hydropower, Sichuan University, Chengdu, 610065, China. ORCID: https://orcid.org/0000-0002-9027-4077. E-mail: wangbo@scu.edu.cn

[2]Master's Candidate, State Key Laboratory of Hydraulics and Mountain River Engineering, College of Water Resource and Hydropower, Sichuan University, Chengdu, 610065, China. E-mail: 1114139373@qq.com

[3]Master's Candidate, State Key Laboratory of Hydraulics and Mountain River Engineering, College of Water Resource and Hydropower, Sichuan University, Chengdu, 610065, China. E-mail: 2078995580@qq.com

[4]Professor, Faculty of Engineering & Informatics, University of Bradford, BD7 1DP, UK. ORCID: http://orcid.org/0000-0002-1653-8441; E-mail: y.guo16@bradford.ac.uk

[5]Professor, State Key Laboratory of Hydraulics and Mountain River Engineering, College of Water Resource and Hydropower, Sichuan University, Chengdu, 610065, China. ORCID: https://orcid.org/0000-0002-9154-231X. E-mail: zhangjianmin@scu.edu.cn

[6]Associate Professor, State Key Laboratory of Hydraulics and Mountain River Engineering, College of Water Resource and Hydropower, Sichuan University, Chengdu, 610065, P. R. China. E-mail: pengyongscu@foxmail.com (Corresponding author)

Abstract: The solutions of dam-break flow mainly developed for the rectangular channels are not applicable to predict the propagation of the dam-break wave in the frictional triangular channels. This study presents an approximate solution considering the frictional effect on the dam-break flow in a dry horizontal triangular channel. The wave tip velocity is solved from an implicit formula about the product of time and resistance coefficient. All other hydraulic properties in the wave tip region

can be expressed as explicit functions of the wave tip velocity. Meanwhile, laboratory experiments have been performed for obtaining the water surface profiles of the dam-break flow from which the position and velocity of the wave tip front have been derived. Results show that the retardation of the wave front position is more significant with the increase of both the resistance and time. The proposed analytical solution shows satisfactory agreement with measurements, suggesting its applicability for predicting the hydraulic properties of the dam-break wave tip in the field situation. It makes feasible to assess analytically the difference between the propagation of the dam-break wave tip in the triangular and rectangular channels.

Keywords: Dam-break; Triangular channel; Wave tip; Hydraulic resistance; Analytical solution.

Introduction

The dam-break flow propagating along a downstream dry bed could be considered as an ideal-fluid flow region (e.g. main flow region) followed by the resistance-dominated wave tip region (Whitham 1955). In the main flow region, the analytical solution can be obtained based on the shallow-water theory, while special treatment for the resistance force acting on water has to be made for obtaining satisfactory predictions in the wave tip region. Dressler (1952) solved the shallow-water equations (SWEs) involving the Chezy resistance term by using a perturbation method. His solution failed in the tip region due to the invalidity of the asymptotic expansions for the first derivatives. Whitham (1955) considered the wave tip region as a definite boundary layer and the velocity in the region as a function of time and developed an approximate solution that became validity for large time or resistance coefficient. Lauber and Hager (1998) presented the determination of the dam-break wave front location under the consideration of the frictional effect. Hogg and Pritchard (2004) developed a new class of similarity solutions containing the bottom resistance for the flow motion in which the drag, inertia and buoyancy had the same magnitude. Chanson (2009) proposed a simple solution for predicting the free-surface profile in the wave tip region by assuming that the fluid mass in the wave tip region was equal to the one in the ideal fluid flow profile. The assumption leads to an

overestimation of the frictional wave front position. Deng et al. (2018) established the relation between the wave tip velocity and time by assuming that the resistance coefficient was constant and the velocity in the wave tip region was uniform. All of the aforementioned analytical models are developed in the rectangular channels, which are not applicable to non-rectangular channels. Both the theoretical and experimental studies have shown that the cross-sectional shape of channels has significant effect on the dam-break wave. Therefore, it is important to understand the hydraulic characteristics of the dam-break wave tip region in non-rectangular channels under the consideration of the bottom resistance, which cannot be obtained from the existing analytical models. To this end, in this study a triangular channel is selected as the non-rectangular one as it is partly the conceptualization of a narrow deep river from the point of view of practice.

To verify the proposed model, accompanying laboratory experiments have been conducted for comparison, because the majority of existing laboratory experiments on dam-break flow were mainly conducted in the rectangular channels (Oertel and Bung 2012; LaRocque et al. 2013; Kocaman and Ozmen-Cagatay 2015). A few measurements were conducted in the triangular flumes. Wang et al. (2019; 2020) performed dam-break flow experiments in a triangular flume with wet bed conditions and focused on the effect of the tailwater depth on the wave propagation Therefore, the influence of hydraulic resistance on the propagation of the dam-break wave tip in the triangular channels still remains unknown. The main objectives of the present study are: (1) to establish an analytical solution for the dam-break wave tip region in the triangular channels following the method of Deng et al. (2018); and (2) to collect measurement data for verifying the proposed model.

Governing Equations for Dam-break Wave Tip Region

The dam-break flow considered here is the flow generated by the sudden and complete release of water initially held at rest behind a vertical plane wall on a dry frictional horizontal triangular channel. All hydraulic parameters are normalized by applying the formulation used by Dressler (1952), i.e., $x = x'/d_o$, $h = h'/d_o$, $u = u'/\sqrt{gd_o}$, $t = t'/\sqrt{d_o/g}$ are used for denoting the

dimensionless distance along the flow direction originated from the dam position, the dimensionless vertical water depth above the bed, the dimensionless depth-averaged flow velocity, and the dimensionless time, respectively, where d_o is initial water depth upstream of the dam site, and x', h', u', t' are used to denote the corresponding dimensional quantities, respectively. Fig. 1 is the sketch of the dam-break wave where x_t and x_f denote the dimensionless positions of the transitional interface and the wave front, respectively. The dimensionless water depth at the transitional interface is denoted as h_t. The dimensionless positions of the frictionless negative and positive wave fronts are $\sqrt{2}t/2$ and $2\sqrt{2}t$, respectively. The frictional force τ_0 is the sidewall shear acting on the wave tip region. Applying the one-dimensional SWEs (Wu et al. 1993) for viscid dam-break flow to an infinitely long prismatic horizontal frictional channel of a triangular cross section, the continuity and momentum equations can be written in the non-dimensional form as:

$$\frac{\partial h}{\partial t}+u\frac{\partial h}{\partial x}+\frac{h}{2}\frac{\partial u}{\partial x}=0 \tag{1}$$

$$\frac{\partial u}{\partial t}+u\frac{\partial u}{\partial x}+\frac{\partial h}{\partial x}+R\frac{u^2}{h}=0 \tag{2}$$

where R = resistance coefficient.

The friction slope in dam-break flow studies is expressed as the Chezy approximation Ru^2/h (Deng et al. 2018), which is included in the momentum equation. For $R = 0$, the exact solution for the ideal-fluid dam-break flow is derived from Eqs. (1)–(2) (Wang et al. 2020):

$$h=\frac{2}{25}\left(2\sqrt{2}-\frac{x}{t}\right)^2;\quad u=\frac{4}{5}\left(\frac{\sqrt{2}}{2}+\frac{x}{t}\right) \tag{3a, b}$$

Eqs. (3a)–(3b) are also valid at the transitional interface connecting the main flow region with the wave tip region because of the continuity of the water depth and flow velocity.

For $R > 0$, the exact solution of Eqs. (1)–(2) cannot be obtained since the Chezy resistance term is nonlinear (Hunt 1987; Chanson 2009). Note that Ru^2/h approaches infinity near the wave front where h approaches zero and it is substantially balanced with the streamwise pressure gradient $\partial h/\partial x$,

as the particle acceleration, i.e., $du/dt = \partial u/\partial t + u\partial u/\partial x$, is expected to be finite. This dominant balance in the wave tip region was used by Whitham (1955), Chanson (2009) and Deng et al. (2018). Thus, Eq. (2) is reduced to

$$\frac{\partial h}{\partial x} + R\frac{u^2}{h} = 0 \tag{4}$$

Based on the assumption of the constant resistance coefficient and the uniform distribution of velocity throughout the wave tip region (Whitham 1955; Chanson 2009; Deng et al. 2018), integrating Eq. (4) yields the momentum equation for the wave tip region:

$$h^2 + 2Ru^2\left(x - x_f\right) = 0 \tag{5}$$

where x_f = dimensionless wave front position along the flow direction originated from dam site. The wave tip velocity is equal to the wave front celerity, namely, $u = dx_f/dt$.

Applying Eq. (5) at the transitional interface yields the dimensionless water depth:

$$h_t = \sqrt{2Ru^2\left(x_f - x_t\right)} \tag{6}$$

Analytical Solution for Dam-break Wave Tip Region

For convenience, two dimensionless variables are introduced as $\tau = Rt$ and $\alpha(\tau) = \left(2\sqrt{2}t - x_f\right)R$, where $\alpha(\tau)$ = dimensionless distance; τ = dimensionless time. The four unknown variables contained in Eq. (6), are then expressed as $x_f = 2\sqrt{2}t - \alpha/R$, $u = 2\sqrt{2} - \dot{\alpha}$, $x_t = \left(2\sqrt{2} - 5\dot{\alpha}/4\right)\tau/R$ and $h_t = \dot{\alpha}^2/8$ using Eqs. (3a, b), where $\dot{\alpha} = d\alpha/d\tau$.

Substituting the expressions of the aforementioned unknown variables into Eq. (6) yields

$$\dot{\alpha}^4 - 32\left(2\sqrt{2} - \dot{\alpha}\right)^2\left(5\tau\dot{\alpha} - 4\alpha\right) = 0 \tag{7}$$

Differentiating Eq. (7) with respect to τ yields:

$$\frac{d\alpha}{d\dot{\alpha}} + \frac{4\alpha}{\dot{\alpha}} = \frac{\left(6\sqrt{2} - \dot{\alpha}\right)\dot{\alpha}^3}{32\left(2\sqrt{2} - \dot{\alpha}\right)^3} \tag{8}$$

Eq. (8) is a first-order linear inhomogeneous equation, whose general solution is expressed as:

$$\alpha = e^{-\int \frac{4}{\dot{\alpha}}\mathrm{d}\dot{\alpha}} \left[\int \frac{\dot{\alpha}^3\left(6\sqrt{2}-\dot{\alpha}\right)}{32\left(2\sqrt{2}-\dot{\alpha}\right)^3} e^{\int \frac{4}{\dot{\alpha}}\mathrm{d}\dot{\alpha}} \mathrm{d}\dot{\alpha} + C \right] \tag{9}$$

where C = integration constant. Integrating Eq. (9) and applying the initial condition (i.e., $\alpha = 0$, $\dot{\alpha} = 0$ at $t = 0$) for determining the integration constant yields:

$$\alpha = \dot{\alpha}^4 \left[\frac{\dot{\alpha}^6}{192} - \frac{3}{16}\dot{\alpha}^4 - \frac{4\sqrt{2}}{3}\dot{\alpha}^3 - 15\dot{\alpha}^2 - 96\sqrt{2}\dot{\alpha} + 192 - 560\ln\left(1-\frac{\dot{\alpha}}{2\sqrt{2}}\right) + \frac{416\sqrt{2}\dot{\alpha}-1536}{\left(2\sqrt{2}-\dot{\alpha}\right)^2} \right] \tag{10}$$

Combining Eqs. (7) and (10) yields:

$$\begin{aligned} \tau = {} & \frac{\dot{\alpha}^3}{160\left(2\sqrt{2}-\dot{\alpha}\right)^2} + \frac{\dot{\alpha}}{240} - \frac{3}{20}\dot{\alpha}^{-1} - \frac{16\sqrt{2}}{15}\dot{\alpha}^{-2} - 12\dot{\alpha}^{-3} \\ & + \frac{128\sqrt{2}}{5}\left[\frac{13}{\left(2\sqrt{2}-\dot{\alpha}\right)^2} - 3\right]\dot{\alpha}^{-4} + \left[\frac{768}{5} - 448\ln\left(1-\frac{\dot{\alpha}}{2\sqrt{2}}\right) - \frac{6144}{5\left(2\sqrt{2}-\dot{\alpha}\right)^2}\right]\dot{\alpha}^{-5} \end{aligned} \tag{11}$$

Eq. (11) is the fundamental solution for the wave tip motion, from which the expressions for the hydraulic properties in the wave tip region can be obtained.

Substituting Eq. (11) in $u = 2\sqrt{2} - \dot{\alpha}$ yields the relation between u and τ:

$$\begin{aligned} \tau = {} & \left(\frac{768}{5} - \frac{6144}{5u^2} + 672\ln 2 - 448\ln u\right)\left(2\sqrt{2}-u\right)^{-5} + \frac{128\sqrt{2}}{5}\left(\frac{13}{u^2}-3\right)\left(2\sqrt{2}-u\right)^{-4} \\ & -12\left(2\sqrt{2}-u\right)^{-3} - \frac{16\sqrt{2}}{15}\left(2\sqrt{2}-u\right)^{-2} + \frac{2}{5\left(1-\sqrt{2}u\right)u^2}\left(2\sqrt{2}-u\right)^{-1} - \frac{u}{96} + \frac{11\sqrt{2}}{240} \end{aligned} \tag{12}$$

For a given resistance coefficient, the wave tip velocity at any time can be determined from Eq. (12) by trial and error method. Applying the value of u in Eqs. (3a, b) yields the dimensionless position and the water depth of the transitional interface:

$$x_t = \left(\frac{5}{4}u - \frac{\sqrt{2}}{2}\right)t \tag{13}$$

$$h_t = \frac{1}{8}\left(2\sqrt{2}-u\right)^2 \tag{14}$$

Substituting Eq. (14) in Eq. (6) produces the dimensionless wave tip length:

$$l = x_f - x_t = \frac{1}{128Ru^2}\left(2\sqrt{2} - u\right)^4 \tag{15}$$

Substituting Eq. (13) in Eq. (15) yields the formula for the dimensionless wave front position:

$$x_f = \left(\frac{5}{4}u - \frac{\sqrt{2}}{2}\right)t + \frac{1}{128Ru^2}\left(2\sqrt{2} - u\right)^4 \tag{16}$$

The water depth profile can then be calculated from Eq. (5) using the values of u and x_f.

The dimensionless total mass of the wave tip region is obtained by using Eq. (5):

$$m = \int_{x_t}^{x_f} \frac{1}{2} h \mathrm{d}x = \int_{x_t}^{x_f} \frac{1}{2}\sqrt{2Ru^2\left(x_f - x\right)}\mathrm{d}x = \frac{\left(2\sqrt{2} - u\right)^6}{3072Ru^2} \tag{17}$$

As the velocity is assumed to be uniform spatially throughout this region, the total momentum of the wave tip region is the product of m and u, expressed as:

$$p = \frac{\left(2\sqrt{2} - u\right)^6}{3072Ru} \tag{18}$$

All of the hydraulic properties except the velocity in the wave tip region can be calculated from explicit formulas, making easy use of the proposed solution. It is feasible to compare analytically the propagation of the dam-break wave tip in the triangular and rectangular channels by using the solutions presented in this study and developed for the rectangular channels. The comparison between the hydraulic properties of the wave tip region in both channels is not provided in this technical note due to the limited space. The analytical results of the water depth, velocity and position of the wave tip front from Eqs. (5), (12) and (17) will be compared with the experimental data in the section "Comparison of Analytical Solution with Experiments".

Laboratory Experiment

Experimental Facility

Dam-break flow experiments have been carried out in a prismatic horizontal flume that is initially dry. As shown Fig. 2, the flume with a triangular cross section is 18 m long, 1 m wide and 1.09 m

high, containing one vertical wall and one inclined wall with angle of 45°. An instantaneous and complete dam break is simulated by suddenly lifting the plate that is located at the distance of 8.37 m from the upstream channel end, resulting in the downstream length of 9.63 m. The plate lifting time for the initial reservoir head of 0.6 m considered in the laboratory test is 0.1875 s, satisfying the criterion for a sudden dam failure (Wang et al. 2019).

Eight high-speed CCD cameras are installed along the flume to record the flow evolution, providing raw images with 1440×1920 pixels with 48 frames per second. One pixel represents the actual length of approximate 1.8 mm. The water surface profiles along the flume are immediately acquired from the recorded flow images by using the digital image processing technique that contains two parts, namely calibration process and water depth acquisition. Both the wave front locations and celerities are derived from the water surface profiles. Fig. 3 shows the flow depth at four locations from two different runs and the scatter plot of measurement. A very good repeatability is found between similar runs.

Determination of Resistance Coefficient

Lauber and Hager (1998) and Chanson (2009) used the individual methods for assessing the resistance coefficient for the wave tip region in the rectangular channels. ASCE Task Committee (1963) reported that the resistance coefficient formula for rectangular channels could be used for non-rectangular channels by adding a correction factor. Analogous to the approach adopted by Lauber and Hager (1998), the resistance coefficient R is determined as $R = (q/\nu)^{-0.1}/40$ where ν = kinematic viscosity (m^2/s); q = discharge per unit width at the dam section (m^2/s), defined for the triangular channels as $q = 256\sqrt{2gd_o^3}/3125$, where g = gravity acceleration (m/s^2); d_o = initial flow depth upstream of the dam (m). For d_o = 0.6 m in the present experiment, the calculated q/ν and R are 1.69×10^5 and 0.0075, respectively.

Comparison of Analytical Solution with Experiments

For understanding the scales of the experiment results more clearly, the values of the normalization

183 parameters are provided as d_o = 0.6 m for both h and x, $(gd_o)^{0.5}$ = 2.4261 m/s for u and $(d_o/g)^{0.5}$ =
184 0.2473 s for t. Fig. 4 shows the experimental images of the evolution of the dam-break flow in the
185 downstream flume. Upon removing the dam, the still water in the reservoir suddenly fell down,
186 generating horizontal jets downstream of the dam (t' = 0.2 s). The upper jet merges rapidly with the
187 lower jet, entrapping air in the water of the wave tip. The flow becomes stable with slight undulation
188 and the water surface slope tends to be mild with time.

189 The measured and predicted water surface profiles in the downstream reach of the flume are
190 compared in Fig. 5, where the dash lines represent the analytical results without bottom resistance. It
191 is demonstrated that the analytical model with R = 0 provides a water surface profile that decreases
192 monotonically from the dam site to the frictionless wave front, being characterized by a concave
193 parabola. It can predict the water depth along the channel except within the wave tip region. The
194 analytical solution considering the resistance coefficient marked by thick grey lines provides the
195 water surface profile of a convex parabola with a vertical tangent at the wave front and generally can
196 capture the water depth variation in the wave tip region. Note that there is a discontinuity of the
197 derivative of the water depth at the transitional interface, which also occurs in the solutions
198 developed by Chanson (2009) and Deng et al. (2018) for the rectangular channels. This is perhaps
199 because the adoption of the same momentum equation, i.e., Eq. (5) is also used in their studies. A
200 discrepancy between experiments and analytical solutions is seen during the initial stage, which
201 should be attributed to the neglect of the significantly vertical water movement in the neighborhood
202 of the dam in the analytical modeling. Both the analytical solutions with R = 0 and R > 0 based on
203 the SWEs are not able to predict the undulation of the water surface.

204 Fig. 6 shows the comparison of the predicted and measured wave front locations. The
205 advancing rate of the wave front position is large during the initial stage and decreases gradually
206 during the later stage. The temporal variation of the wave front locations is well predicted by the
207 model considering the bottom resistance, except a visible discrepancy in the near-field area that leads

to a moderate value of the relative root mean square error (RRMSE = 29.08 %) between measurements and analytical solutions. The deviation of the analytical solution without resistance from the measurements becomes larger with time, indicating that the hydraulic resistance retards the wave front position more significantly by with increasing time. If the bottom resistance is not considered, the wave front positions equal $2\sqrt{2t}$ (dash line), whose trajectory is a straight line.

Fig. 7 shows the comparison between the measured and predicted wave tip velocities in the triangular channels. The experimental observation shows that the wave tip velocity decreases sharply at the initial stage (i.e., about $t < 5$) and then declines gradually. The analytical solution with bottom resistance provides a monotonically descent curve for the velocity with an initial value of $u = 2\sqrt{2}$ at $t = 0$ and satisfactorily agrees with the measurements with a small value of RRMSE = 3.21 %. If the bottom resistance is absent, a constant velocity of $2\sqrt{2}$ is produced, dramatically different from the measurements. Furthermore, the discrepancy between the analytical solution with $R = 0$ and the experimental data increases as time goes, indicating that the retardation of bottom resistance has an accumulative effect.

The above comparison shows that the analytical solution with the determination of the resistance coefficient for the triangular channel has good agreement with the experimental measurements in the wave tip region, verifying the rationality of the dominant balance between the pressure gradient and the friction near the wave tip. Beyond the wave tip region, the analytical solution neglecting resistance effects provides a satisfactory result for the water depth variation except the undulation that will attenuate with time. This study confirms that the widely adopted treatment that divides the entire domain into an ideal-fluid flow region and a resistance-dominated wave tip region for the rectangular channel is also valid for non-rectangular channels, e.g., the triangular channels considered in the present study. The incorporation of the analytical solutions with $R > 0$ and $R = 0$ for the two flow regions makes it feasible to predict the hydraulic properties in the entire domain.

Conclusions

An analytical solution has been developed for the dam-break wave tip region on a dry frictional channel with a triangular cross section in the study. The wave tip velocity is expressed as an implicit function of the product of time and resistance coefficient, while all other hydraulic properties including wave front position, wave tip length, water depth, mass and momentum of wave tip region have explicit formulas with regard to the wave tip velocity. Experimental measurements of dam-break flows are conducted in a prismatic horizontal flume with a triangular cross section, which are used for verifying the analytical model.

The solution shows that the retardation effect of the bottom resistance on the velocity and location of the wave tip front becomes more significant as time elapses, which cannot be predicted by the method without consideration of the bottom resistance. It is found that the derivative of the water depth provided by the presented solution is not continuous at the transitional interface, which may be caused by the derivation of the presented solution only from the momentum equation.

The proposed model compares well with the experimental data including the water surface profile, the location and velocity of the wave front, demonstrating the applicability of the analytical model for predicting the hydraulic properties in the wave tip region in actual situation. The proposed approach can provide a satisfactory approximation of R for the triangular channels.

Data Availability Statement

Some or all data, models, or code generated or used during the study are available from the corresponding author by request (analytical and experimental test data in the form of Excel).

Acknowledgements

This study is supported by the National Natural Science Foundation of China (Grant No: 51879179, 52079081).

Notation

The following symbols are used in this note:

C = integration constant;

d_o = initial flow depth upstream of the dam;

g = gravity acceleration;

h = dimensionless flow depth;

h' = dimensional flow depth;

l = dimensionless wave tip length;

m = dimensionless mass;

p = dimensionless momentum;

q = discharge per unit width at the dam section;

R = resistance coefficient;

t = dimensionless time;

t' = dimensional time;

u = dimensionless average flow velocity;

u' = dimensional average flow velocity;

x = dimensionless position;

x' = dimensional position;

α = dimensionless distance;

τ = dimensionless time;

τ_0 = boundary shear stress; and

v = kinematic viscosity of water.

Subscripts

f = wave front; and

t = transitional interface.

References

ASCE Task Force of Hydrodynamics Committee, 1963. “Friction Factors in Open Channels”: *J.*

283 *Hydraul. Div*. 89(2): 97–143.
284 Chanson, H. 2009. “Application of the method of characteristics to the dam break wave problem.” *J.*
285 *Hydraul. Res*. 47(1): 41–49. https://doi.org/10.3826/jhr.2009.2865
286 Deng, X.H., H.J. Liu, and S.X. Lu. 2018. “Analytical study of dam-break wave tip region.” *J.*
287 *Hydraul. Eng.* 144(5): 04018015. https://doi.org/10.1061/(ASCE)HY.1943-7900.0001453
288 Dressler, R. F. 1952. “Hydraulic resistance effect upon the dam-break functions.” *J. Res. Natl. Bur.*
289 *Stand*. 49(3): 217–225.
290 Hogg, A. J., and D. Pritchard. 2004. “The effects of hydraulic resistance on dam-break and other
291 shallow inertial flows.” *J. Fluid Mech*. 501: 179–212.
292 https://doi.org/10.1017/S0022112003007468
293 Hunt, B. 1987. “An inviscid dam-break solution.” *J. Hydraul. Res*. 25(3): 313–327.
294 http://dx.doi.org/10.1080/00221688709499273
295 Kocaman, S., and H. Ozmen-Cagatay. 2015. “Investigation of dam-break induced shock waves
296 impact on a vertical wall.” *J. Hydrol*. 525: 1–12. https://doi.org/10.1016/j.jhydrol.2015.03.040
297 LaRocque, L., J. Imran, and M. Chaudhry. 2013. “Experimental and numerical investigations of
298 two-dimensional dam-break flows.” *J. Hydraul. Eng*. 139(6): 569–579.
299 https://doi.org/10.1061/(ASCE)HY.1943-7900.0000705
300 Lauber, G., and W. H. Hager. 1998. “Experiments to dambreak wave: horizontal channel.” *J. Hydraul.*
301 *Res*. 36(3): 291-307. https://doi.org/10.1080/00221689809498620
302 Oertel, M., and D. B. Bung. 2012. “Initial stage of two-dimensional dam-break waves: laboratory
303 versus VOF.” *J. Hydraul. Res*. 50(1): 89–97. https://doi.org/10.1080/00221686.2011.639981
304 Wang, B., J. M. Zhang, Y. L. Chen, Y. Peng, X. Liu, and W. J. Liu. 2019. “Comparison of measured
305 dam-break flood waves in triangular and rectangular channels.” *J. Hydrol*. 575: 690–703.
306 https://doi.org/10.1016/j.jhydrol.2019.05.081.
307 Wang, B., X. Liu, J. M. Zhang, Y. K. Guo, Y. L. Chen, Y. Peng, W. J. Liu, S. Yang, and F. J. Zhang.

2020. “Analytical and experimental investigations of dam-break flows in triangular channels with wet-bed conditions.” *J. Hydraul. Eng.* 146(10): 04020070. https://doi.org/10.1061/(ASCE)HY.1943-7900.0001808.

Whitham, G. B. 1955. “The effects of hydraulic resistance in the dam-break problem.” *Proc. R. Soc. London*. 227(1170): 399–407.

Wu, C., G. Q. Dai, and C. G. Wu. 1993. “Model of dam-break floods for channels of arbitrary cross section.” *J. Hydraul. Div.* 119(8): 911–923. https://doi.org/10.1061/(ASCE)0733-9429(1993)119:8(911)

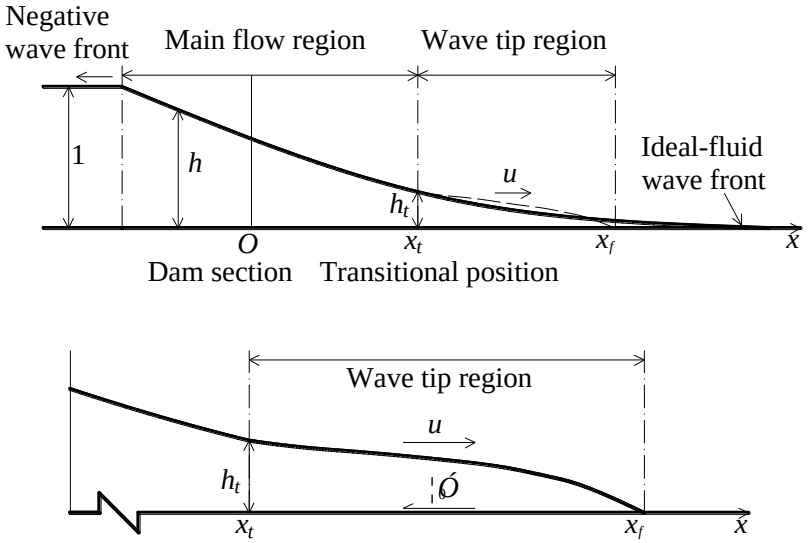

Fig. 1. Dam-break wave in a dry horizontal channel.

Fig. 2 (Color) Physical model for simulating dam-break flow viewed from the left. The yellow plate represents the dam (red arrow). The right sidewall is white with an inclined angle of 45°; the left sidewall is transparent and vertical. The cameras (light blue arrow) are mounted on the metal bars fixed outside the left sidewall.

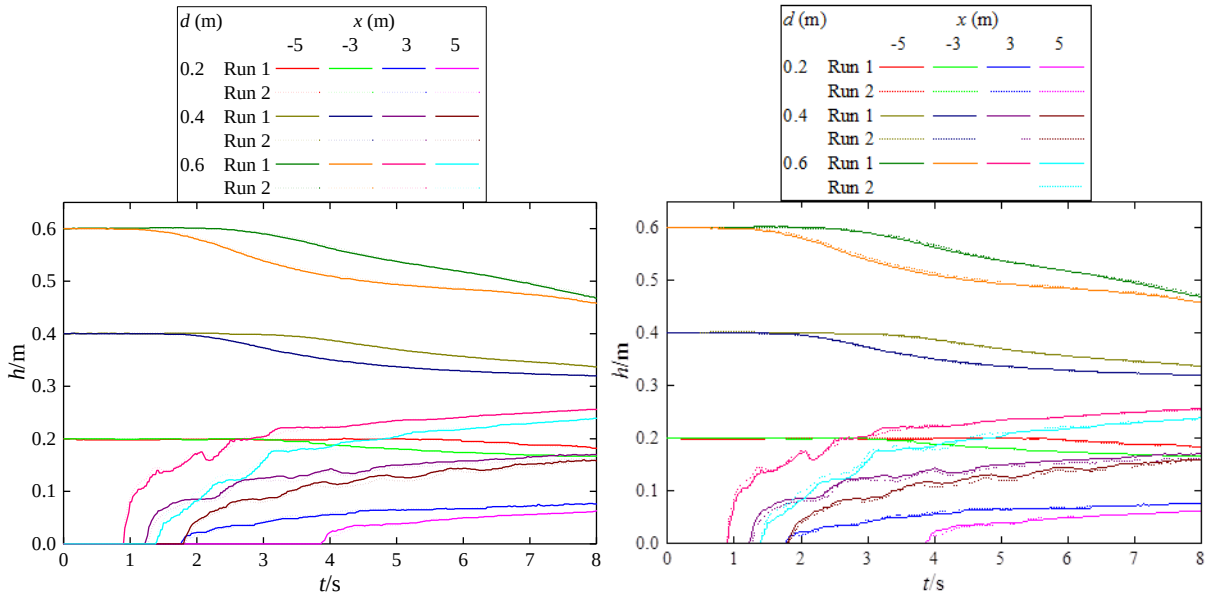

(a) (b)

Fig. 3. Repeatability of water depth measurement: (a) location x = −5, −3, 3 and 5 m; (b) repeatability scatter plot.

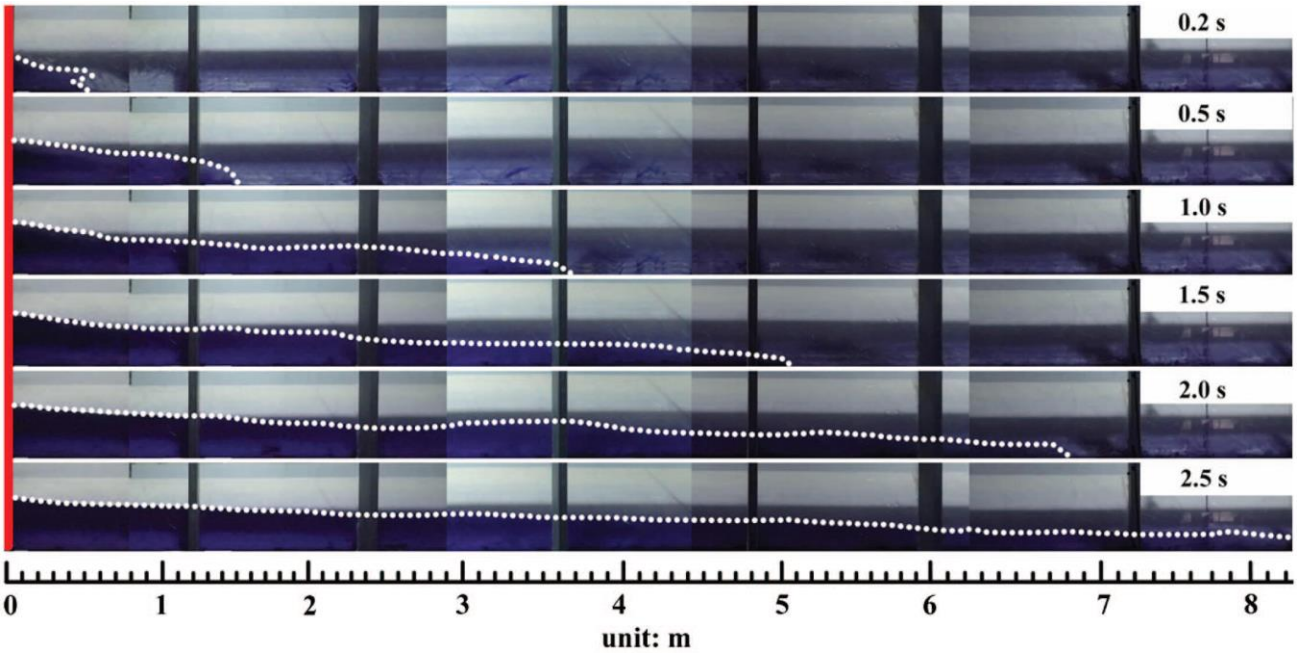

329 Fig. 4. Experimental images of the flow in the downstream flume. The dam site is indicated with a

330 red line.

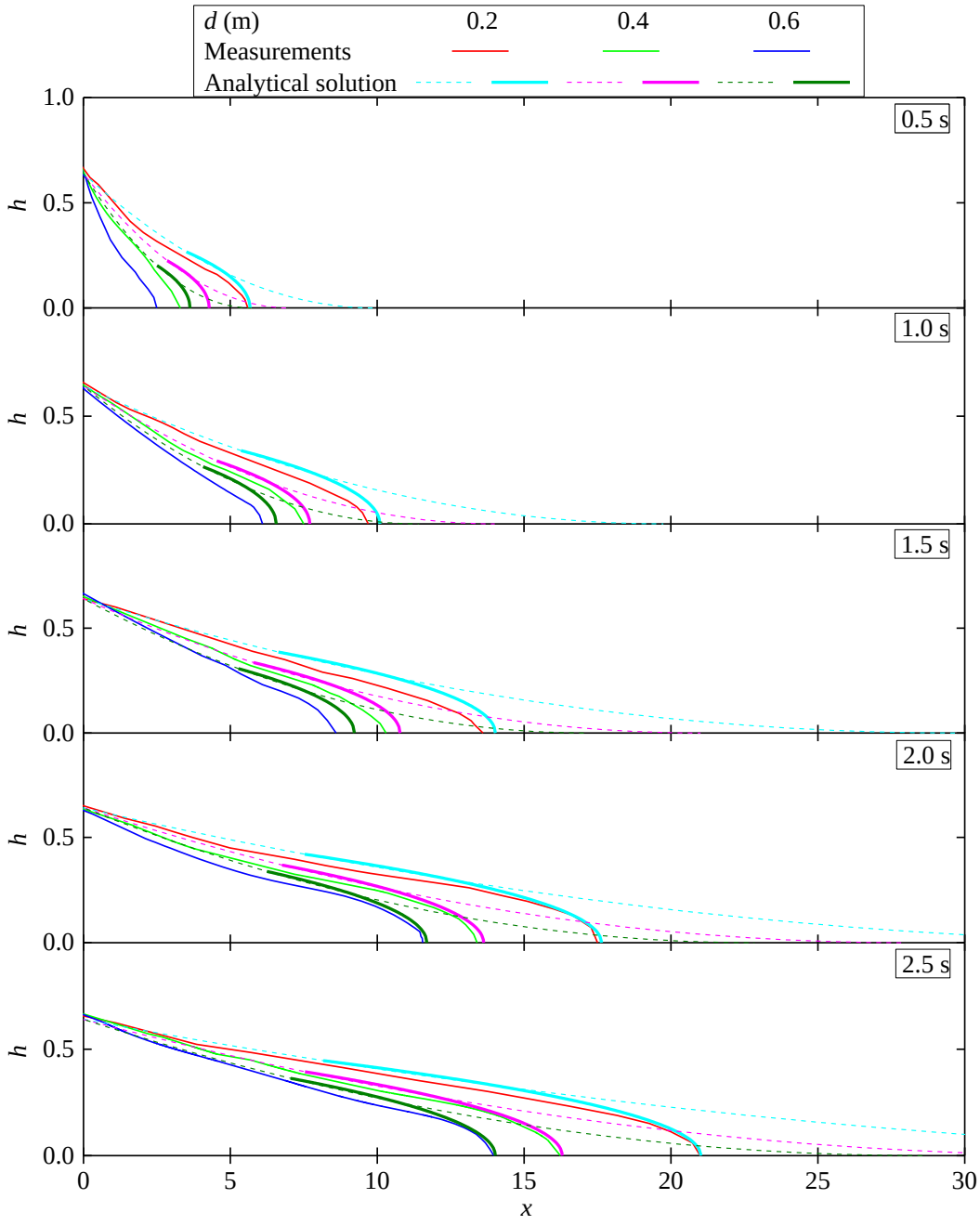

331

332 Fig. 5. Comparison between measured water surface profiles and analytical solutions. The dashed

333 line indicates the analytical solution with R = 0 and the thick grey line is for R > 0.

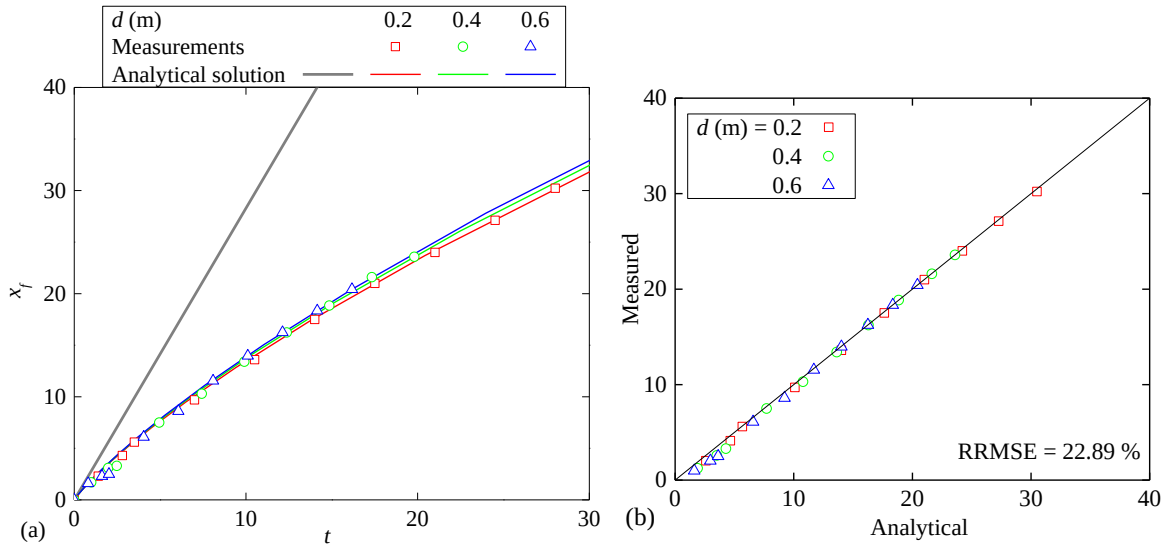

Fig. 6. Wave front locations: (a) measurements and analytical solutions; (b) measurement versus analytical solution. The dashed line indicates the analytical solution with R = 0.

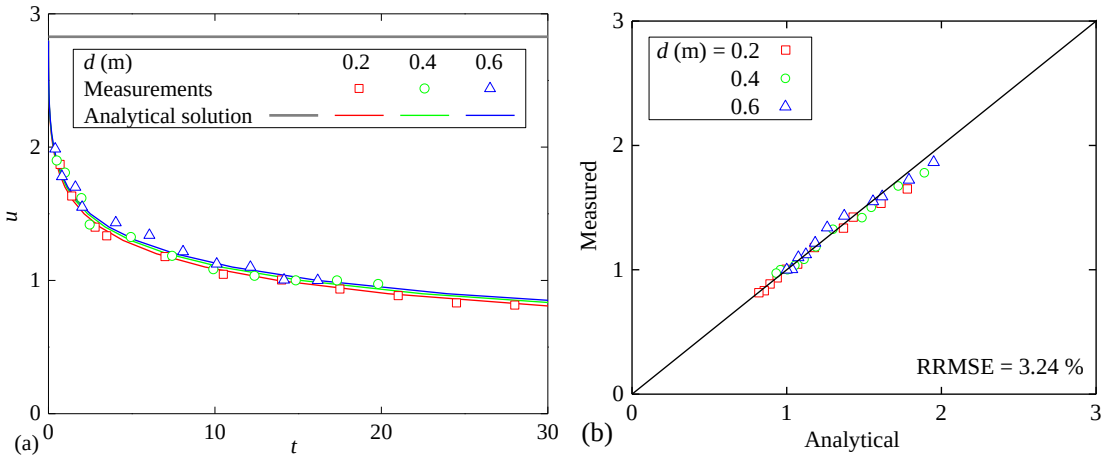

Fig. 7. Wave tip velocities: (a) measurements and analytical solutions; (b) measurement versus analytical solution.